

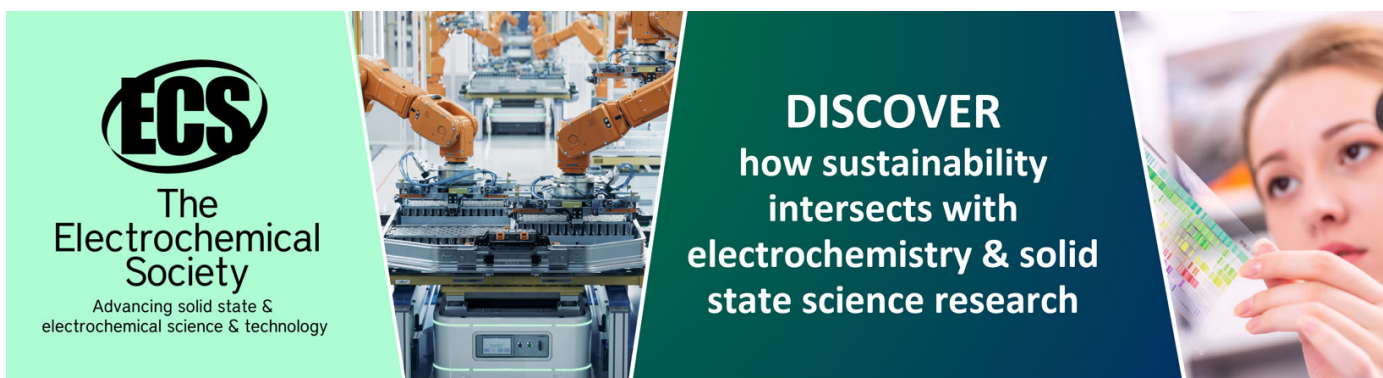
Hydrophobic metallic nanorods with Teflon nanopatches

To cite this article: Wisam J Khudhayer *et al* 2009 *Nanotechnology* **20** 275302

View the [article online](#) for updates and enhancements.

You may also like

- [Microfabrication of a digital microfluidic platform integrated with an on-chip electrochemical cell](#)
Yuhua Yu, Jianfeng Chen, Jian Li et al.
- [Optimization of the Microstructure of the Cathode Catalyst Layer of a PEMFC for Two-Phase Flow](#)
Roland Friedmann and Trung Van Nguyen
- [Ionomer Segregation in Composite MEAs and Its Effect on Polymer Electrolyte Fuel Cell Performance](#)
Jian Xie, Fernando Garzon, Thomas Zawodzinski et al.



ECS
The
Electrochemical
Society
Advancing solid state &
electrochemical science & technology

DISCOVER
how sustainability
intersects with
electrochemistry & solid
state science research

Hydrophobic metallic nanorods with Teflon nanopatches

Wisam J Khudhayer, Rajesh Sharma and Tansel Karabacak

Department of Applied Science, University of Arkansas at Little Rock, AR 72204, USA

E-mail: wjkhudhayer@ualr.edu

Received 21 February 2009, in final form 13 May 2009

Published 16 June 2009

Online at stacks.iop.org/Nano/20/275302

Abstract

Introducing a hydrophobic property to vertically aligned hydrophilic metallic nanorods was investigated experimentally and theoretically. The platinum nanorod arrays were deposited on flat silicon substrates using a sputter glancing angle deposition technique (GLAD). Then a thin layer of Teflon (nanopatch) was partially deposited on the tips of platinum nanorods at a glancing angle of $\theta_{\text{dep}} = 85^\circ$ for different deposition times. Teflon deposition on Pt nanorods at normal incidence ($\theta_{\text{dep}} = 0^\circ$) was also performed for comparison. Morphology and elemental analysis of Pt/Teflon nanocomposite structures were carried out using scanning electron microscopy (SEM) and energy dispersive x-ray analysis (EDAX), respectively. It was found that the GLAD technique is capable of depositing ultrathin isolated Teflon nanostructures on selective regions of nanorod arrays due to the shadowing effect during obliquely incident deposition. Contact angle measurements on nanocomposite Pt nanorods with Teflon nanopatches exhibited contact angle values as high as 138° , indicating a significant increase in the hydrophobicity of originally hydrophilic Pt nanostructures that had an angle of about 52° . The enhanced hydrophobicity of the Pt nanorod/Teflon nanopatch composite is attributed to the presence of nanostructured Teflon coating, which imparted a low surface energy. Surface energy calculations were performed on Pt nanorods, Teflon thin film, and Pt/Teflon composite using the two-liquid method to confirm the contact angle measurements. Furthermore, a new contact angle model utilizing Cassie and Baxter theory for heterogeneous surfaces was developed in order to explain the enhanced hydrophobicity of Pt/Teflon nanorods. According to our model, it is predicted that the solid-liquid interface is mainly at the Teflon tips when the composite nanorods are in contact with water.

(Some figures in this article are in colour only in the electronic version)

1. Introduction

Fluorocarbon thin film coatings have attracted much attention due to their favorable electrical, chemical, and surface properties [1–3]. Plasma deposition of fluorocarbon polymers using radio-frequency (RF) sputtering has been investigated since 1969 [4–8]. In recent years interest in RF sputtering of fluorocarbon polymers has been renewed [9], as the plasma deposited polymer films are again in demand as protective, low friction, and non-wettable coatings. Polytetrafluoroethylene (PTFE), commonly known as Teflon, has been the focus of the majority of the studies in this area [9–15].

Among its various properties, some of the important features of PTFE are that (1) it is a chemically inert and easily available material [13], (2) PTFE can be cast into

different shapes [13], and (3) it has a low surface energy with a contact angle of water around 105° [1, 10] for bulk Teflon and can be made as high as 165° through various surface processing techniques [14, 15]. Because of these advantages, superhydrophobic surfaces (i.e. contact angle values exceeding 150°) made out of Teflon have attracted much interest in many practical applications. Some of the recent applications include removing surface contaminations and as an industrial water repellent [9, 13].

It has been reported that an increase in PTFE film surface roughness increases the contact angle of water and therefore hydrophobicity without altering the surface chemistry [14, 15]. Recently, Satyaprasad *et al* [14] reported depositing Teflon-like superhydrophobic coatings on stainless

steel. In their work, Teflon tailings were pyrolyzed to generate fluorocarbon precursor molecules, and an expanding plasma arc (EPA) was used in order to polymerize these precursors to deposit the Teflon-like coating. It was found that the coatings had a rough cauliflower morphology at substrate temperatures lower than 100° and a dense smoother morphology at higher temperatures. The rough coatings showed superhydrophobic behavior with a water contact angle of 165° . In another recent work, a contact angle as high as 164° has been measured on RF-sputtered rough Teflon thin films coated on aluminum substrates, where the Al was pre-etched to form a rough template for the subsequent Teflon deposition [15]. In both studies, the resulting Teflon coating was a continuous rough film that enhanced the hydrophobicity. In addition, some researchers also studied modifying surface chemistry through approaches such as the anodic oxidation of aluminum surfaces [16] and the sol-gel process [17] in order to increase the hydrophobicity. Recently, single crystalline silver dendrites were grown on a Ni/Cu substrate by utilizing a simple templateless and surfactantless electrochemical technique in AgNO_3 solution [18]. In this study, the deposited silver morphology was changed from polyhedrons to dendrites by controlling the applied potential. The silver dendritic film/substrate with thickness of about $10\ \mu\text{m}$ was modified with a self-assembled monolayer of n-dodecanethiol. It has been shown that the modified dendritic silver film with a monolayer of n-dodecanethiol yields a superhydrophobic surface with a contact angle of 154.5° . The superhydrophobicity has been generally attributed to the combined effects of roughening in surface morphology and changes in surface chemistry [15].

However, as the micro- and nanotechnology based systems quickly emerge, conventional continuous PTFE coatings that completely cover the underlying surface may block the desired transfer of photons/atoms/particles from/to the outside environment. Therefore, some applications may require 'hydrophobic yet still isolated not fully coated nanostructured surfaces'. As an example, it can be desirable to have hydrophilic arrays of nanostructures that are only partially coated with Teflon nanopatches at their tips, which allows the underlying material to be exposed to the outside environment and perform its function as the Teflon at the tips introduces the hydrophobic property. Therefore, the final multifunctional composite nanostructure becomes a chemically hydrophobic material. Although there are many important applications for such nanostructures in surface catalysis, hydrogen production/storage, and heat transfer, there is no previously reported study of controlling the hydrophilicity/hydrophobicity of metallic nanostructures/microstructures through nanocomposite coating approaches.

In this study, a novel glancing angle deposition (GLAD) technique was used to deposit ultrathin isolated Teflon nanostructures selectively on the tips of platinum (Pt) nanorods. The GLAD technique provides a novel capability for growing 3D nanostructure arrays with interesting material properties [18–21]. It is a simple, single-step process unlike the surface roughening and surface modification approaches mentioned above. In addition, GLAD offers a cost and time

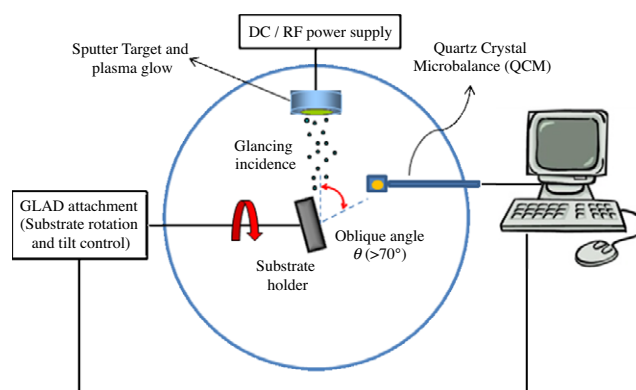


Figure 1. Schematic of our GLAD system that allows deposition of different materials.

efficient method to fabricate nanostructured arrays of almost any material in the periodic table as well as alloys and oxides. The GLAD technique uses the 'shadowing effect,' which is a 'physical self-assembly' process through which obliquely incident atoms/molecules can only deposit to the tops of higher surface points, such as to the tips of a nanostructured array or to the hill tops of a rough or patterned substrate. We show that the contact angle of the composite structure of Pt nanorods with Teflon nanopatches at the tips dramatically increases from hydrophilic values of uncoated nanorods to the highly hydrophobic values after coating with Teflon tips.

2. Experimental details

A schematic of the custom-made GLAD experimental setup in the present study is shown in figure 1. Our GLAD setup has been constructed by our group. However, some of the components including DC and RF magnetrons were supplied by Excel instruments (India). In our experiments, a DC magnetron sputtering system was employed for the fabrication of Pt nanorod arrays. The depositions were performed on native oxide p-Si (100) wafer pieces (substrate size $3 \times 3\ \text{cm}^2$), using a 99.99% pure Pt cathode (diameter about 7.6 cm). The substrates were mounted on a sample holder located at a distance of about 18 cm from the cathode. They were tilted so that the angle between the surface normal of the target and the surface normal of the substrate was $\theta_{\text{dep}} = 85^\circ$. The substrates were rotated around the surface normal with a speed of 30 RPM. The base pressure of about 4×10^{-7} Torr was achieved using a turbo-molecular pump backed by a mechanical pump. In all deposition experiments, the power was 200 W with an ultrapure Ar working gas pressure of 2.0×10^{-3} Torr. The substrate temperature during growth was below $\sim 85^\circ\text{C}$. The deposition time was 60 min. The deposition rate of the glancing angle depositions of Pt nanorods was measured utilizing quartz crystal microbalance (Inficon-Q-pod QCM monitor, crystal: 6 MHz gold coated standard quartz) measurements and SEM image analysis to be about $10\ \text{nm}\ \text{min}^{-1}$. First, the deposition rate of Pt nanorods was monitored on the QCM. Since the distance between the target and the QCM is smaller than that of the substrate, the

deposition rate of Pt nanorods on the substrate was determined by dividing the measured film thickness from cross-sectional SEM images by the deposition time. Then, a correction distance factor was calculated dividing the deposition rate on the substrate to that on the QCM. Finally, using this factor and QCM readings in the subsequent depositions, the exact deposition rate of Pt nanorods on the substrate was determined *in situ*.

After fabricating Pt nanorods, Teflon was deposited on top of Pt nanorods by utilizing an RF sputter deposition at a glancing angle of $\theta_{\text{dep}} = 83.7^\circ$ (GLAD) for different deposition times of 1, 5, 15, and 30 min. For the normal incidence ($\theta_{\text{dep}} = 0^\circ$), the deposition times were 20 s and 5 min. GLAD allows coating Teflon only on the tips of the Pt nanorods, resulting in a bi-layer nanorod structure (Pt base and Teflon tip), while normal incidence results in a continuous Teflon thin film coating. A custom-made Teflon (Applied Plastics Technology) disk was used as the sputtering target. The target was 0.3175 cm thick and 5.08 cm in diameter. The substrates (arrays of Pt nanorods on a silicon wafer piece) were rotated around the surface normal with a speed of 1 RPM. The deposition was performed under a base pressure of about 4×10^{-7} Torr. During Teflon deposition experiments, the power was 150 W with an ultrapure Ar working gas pressure of 3.2×10^{-3} Torr. In a similar fashion to the Pt nanorods, the deposition rates of the normal incidence and glancing angle depositions of Teflon nanopatches were measured using SEM image analysis and QCM measurements to be about 13 and 4 nm min⁻¹, respectively. The surface morphology of the nanocomposite (Pt/Teflon) structures was analyzed using an SEM. Furthermore, elemental chemical analysis was performed using an EDAX system, which was attached to the SEM unit. In addition, the hydrophobic behavior was investigated by contact angle measurements using a VCA optima surface analysis system (AST Products, Inc., MA). Finally, the surface energy measurements were also performed using the two-liquid method to confirm the contact angle measurements.

3. Results and discussion

3.1. Surface morphology: SEM measurements

A scanning electron microscopy (SEM) unit (FESEM-6330F, JEOL Ltd, Tokyo, Japan) was used to study the morphology of our multifunctional composite (Pt/Teflon) nanostructures. Figure 2 shows the SEM images of pure Pt nanorods and the composite structure of Pt nanorods with Teflon tips which are deposited using the RF sputtering technique at a glancing angle as well as at normal incidence for different deposition times. It was challenging to get clear SEM images of Pt/Teflon composites due to the charging of the Teflon surface. However, this charging helped us to locate the Teflon coated regions on the Pt nanorods, which were visualized as a whitish coating in cross-sectional SEM images. The Teflon film thickness was determined as follows: first, we located the center of the individual nanotip of the Pt nanorods utilizing cross-sectional SEM image analysis. Then we drew a line at the top portion

Table 1. Measured contact angle values for various Teflon deposition times and Teflon thicknesses using either the normal incidence (capping) or glancing angle deposition (GLAD-nanopatches) technique are listed.

Sample number	Sputtering mode	Deposition time	Teflon thickness (nm)	Contact angle (deg)
1	Normal incidence (capping)	20 s	4	130
2	Normal incidence (capping)	5 min	64	122
3	GLAD-nanopatches	1 min	4	138
4	GLAD-nanopatches	5 min	21	135
5	GLAD-nanopatches	15 min	64	133
6	GLAD-nanopatches	30 min	128	132

of the selected nanotip which was parallel to the bottom plane. Finally, Teflon film thickness was determined starting from the line drawn up to the end of the Teflon film. From SEM images, it was found that the GLAD technique was able to deposit Teflon selectively on the tips of Pt nanorods, which results in isolated arrays of composite nanostructures. On the other hand, conventional normal incidence deposition of Teflon on Pt nanorods resulted in a continuous Teflon capping thin film layer lying mainly at the tips of Pt nanorods. We also observed that, as the deposition time increases, Teflon islands tend to coalesce with other Teflon islands on neighboring nanorods in both normal incidence and GLAD depositions, which results in a smoother Teflon surface at the top and a decrease in the contact angle values. In general, for normal angle deposition, coalescence of Teflon islands is more pronounced, film quickly gets smoother, and therefore contact angle values decrease faster compared to the GLAD-Teflon as shown in table 1.

3.2. Elemental analysis and mapping of Pt/Teflon nanocomposite

Energy dispersive x-ray analysis (EDAX) was utilized for elemental analysis and mapping of Pt/Teflon composites (samples 2 and 4 in table 1). EDAX analysis (not shown) reveals that the elements present in our composite samples are carbon, fluorine, platinum, and silicon. The true carbon to fluorine ratio for a chemical composition analysis of the Teflon layer cannot be determined from EDAX plots due to the carbon contamination in the EDAX chamber. In addition, figure 3 shows the spatial distribution of fluorine atoms mapped for GLAD and normal incidence deposited Teflon on Pt nanorods, respectively. Although the fluorine atoms boundaries were not well defined due to the size of the EDAX beam, which is about 100 nm, it can be seen from figure 3(a) that the density of fluorine at the tips of Pt nanorods is higher than that at the gaps. This indicates that Teflon is concentrated on the tips of Pt nanorods when it is deposited by GLAD. This result further

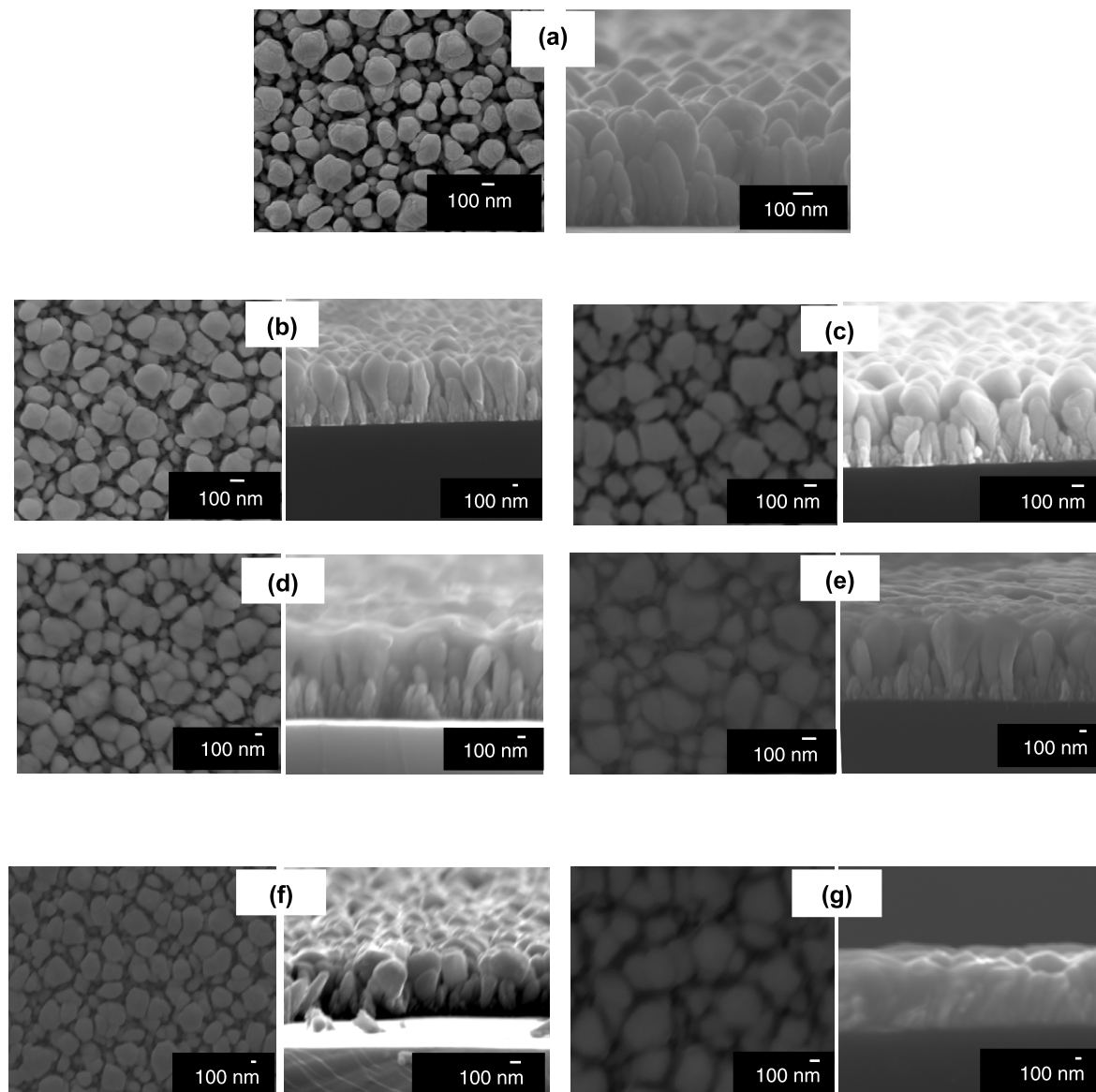


Figure 2. Top and cross-section views of bare glancing angle deposition (GLAD) Pt nanorods (a), Pt nanorods with GLAD-Teflon nanopatches at the tips for different deposition times of 1 (b) (ultrathin Teflon deposition was made for 1 min), 5 (c), 15 (d), and 30 (e) min, respectively, and Pt nanorods with normal incidence—Teflon film for different deposition times of 20 seconds (f) and 5 min (g), respectively.

supports our SEM image analysis and shows that GLAD is capable of producing isolated composite nanostructures.

On the other hand, for normal incidence deposition of Teflon, the distribution of fluorine atoms in figure 3(b) is relatively more uniform on the Pt nanorods and in the gaps compared to the GLAD-Teflon in figure 3(a). Relatively higher fluorine density at the tips for normal incidence deposited Teflon is attributed to the still present shadowing effect in the sputter flux, which has a cosine type angular distribution [22]. Angular distribution of the incident flux is related to the argon pressure used; the higher the argon pressure, the higher the angular distribution is. The angular distribution drives some of the arriving atoms to land on the substrate at oblique angles rather than the normal angle. Since gaps among the nanorods are small, the angular distribution may cause obliquely arriving atoms to deposit at the tips of the nanorods and plug the gaps over time due to the lateral growth. Normally incident fluorine

atoms can still penetrate through gaps before they are closed up, leading to a more uniform coating of nanorods compared to GLAD-Teflon that produces nanopatches only at the tip regions. However, during GLAD-Teflon, it is possible that some side walls of some Pt nanorods were partially coated with a few nanometer thick layer of Teflon due to the angular distribution of the incident flux. During GLAD, angular distribution this time leads to a small portion of atoms coming in at smaller deposition angles that allow them to reach to the upper portion of nanorod sidewalls.

3.3. Contact angle measurements and modeling

Contact angle measurements were performed for characterization of bare Pt nanorods, conventional flat Teflon thin film, Pt nanorods coated with normal incidence deposited Teflon film, and Pt nanorods with ultrathin GLAD-Teflon tips

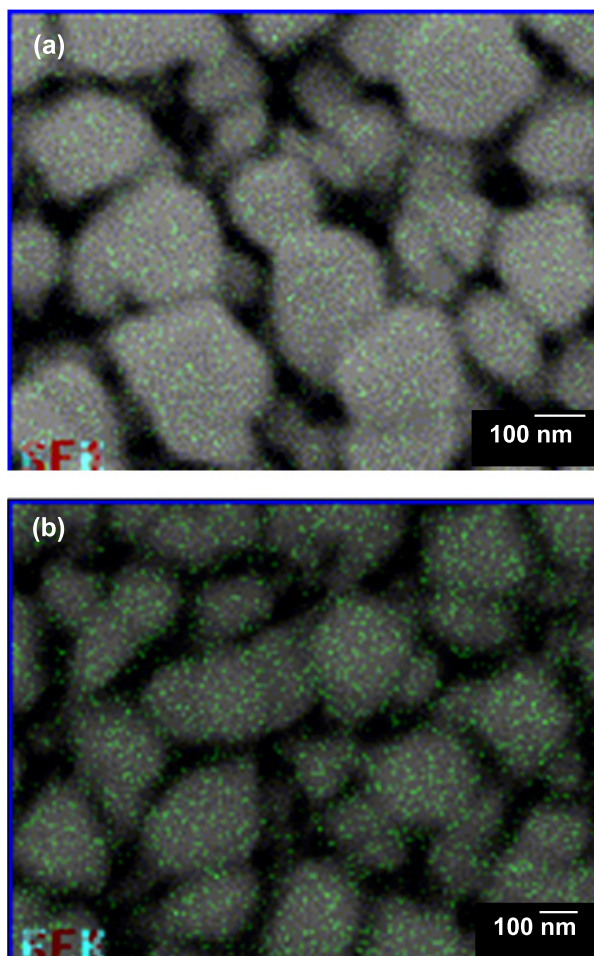


Figure 3. EDAX elemental distribution of fluorine is mapped over the SEM images of Pt/Teflon composite: (a) Teflon nanopatches were produced by GLAD for a deposition time of 5 min and (b) Teflon was deposited by conventional normal angle deposition for a growth time of 5 min.

(nanopatches) using a VCA Optima surface analysis system. In the literature, the term ‘ultrathin’ films means that the thickness of the films is less than about 5 nm [15]. The contact angle measurement is a simple experiment where the image of a water droplet on a given substrate is captured and the angle that traces the air–water to water–substrate interface is measured from the origin of the air–water–substrate contact point at the edge. This contact angle larger than 90° denotes a hydrophobic surface and gets close to 180° for superhydrophobic surfaces, resulting in a spherical water droplet. The contact angle measurements of Pt nanorods, Teflon thin film, and Pt nanorods coated with Teflon tips are shown in figure 4. It is well known that substances such as Pt and Teflon exhibit different behavior when their surfaces get in contact with a water droplet. It was found that the average contact angle of Pt nanorods was about 52° , as shown in figure 4(a), indicating a hydrophilic surface. This value is comparable with the previously reported contact angle of Pt nanorods [23]. Similarly, for the normal angle deposited flat Teflon thin film, the average contact angle was about 108° (see figure 4(b)), which indicates a hydrophobic surface, and it is in close agreement with the previously reported values of the contact angle of Teflon films [1, 10].

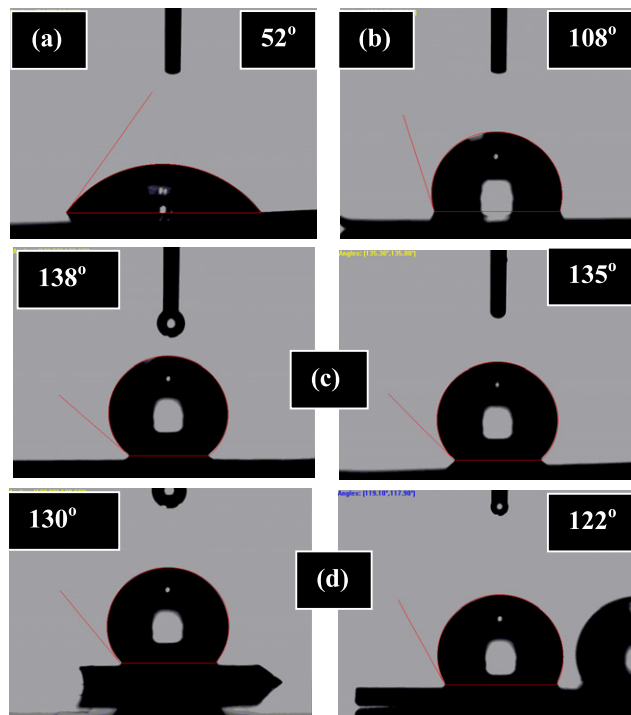


Figure 4. Contact angle measurements of (a) Pt nanorods, (b) Teflon thin film, (c) Pt nanorods with glancing angle deposited (GLAD) Teflon tips for different deposition times of 1 and 5 min, and (d) Pt nanorods with normal incidence deposited Teflon capping for different deposition times of 20 s and 5 min.

As can be seen from table 1, higher contact angle values of composite (Pt/Teflon) have been measured, indicating a significant increase in the hydrophobicity of originally hydrophilic Pt nanostructures. This newly imparted hydrophobicity of nanorods may be attributed to the presence of low surface energy Teflon nanopatches with large surface area, as can be observed in the SEM images shown in figure 2. The relatively lower contact angle of Pt/Teflon composite (about $130\text{--}140^\circ$) compared to the previously reported values (165°) in the literature [14, 15] is likely due to the competition between the hydrophilic Pt nanorod base and the hydrophobic Teflon patches at the nanorod tips. However, the previously reported contact angles may also originate from different surface roughness values and differences in Teflon composition (i.e. carbon to fluorine ratio) compared with those of our Pt/Teflon nanocomposite surfaces.

In order to better understand the wetting of composite nanorods, a simplified two dimensional model (figure 5) has been developed utilizing Cassie and Baxter theory [24] of partial wetting of rough surfaces that leads to a heterogeneous interface formed by contacts of solid and vapor (air) with the liquid. In our model illustrated in figure 5, d represents the water depth measured from the tip of the nanorods, a is the diameter of the nanorods, b is the gaps among the nanorods, t is the portion of Teflon at the side walls of the nanorods starting from the base line of the nanorod tips, and α is the tilt angle of the facets of the nanotips measured from the line parallel to the bottom plane. The average diameter of the nanorods is around 150 nm, which is measured from the SEM images. Under the

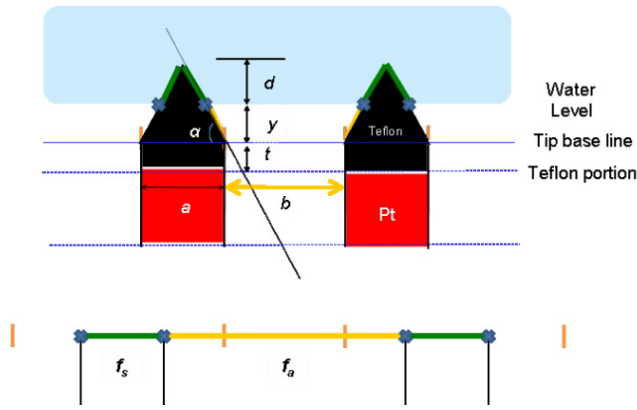


Figure 5. Cross-section of the simplified wetting model on Pt/Teflon nanocomposite. The composite surface is flattened so that the Cassie and Baxter theory can be applied to predict the composite contact angle.

Cassie and Baxter assumption, the fluid forms a composite surface with the solid where the water droplet sits upon a composite surface of the solid tops and the air gaps, alternating between a fluid–solid interface and a fluid–vapor interface. Therefore, the Wenzel’s model [23, 24], which assumes that the fluid completely wets the solid structure, was modified by introducing the fractions f_s and f_a , which correspond to the area in contact with the liquid and the area in contact with the trapped air beneath the drop, respectively [24]:

$$\cos \theta_{CB} = f_s \cos \theta_Y + f_a - 1 \quad (1)$$

where θ_Y is the contact angle that a liquid drop makes with an ideally flat surface (Young’s theory) and f_s is the area fraction of the solid–fluid interface. As can be seen from equation (1), if f_s tends to zero the contact angle approaches 180° , and as f_s tends to one the expression tends to the Wenzel’s equation. In our model, the nanostructured surface is flattened so that the water droplet sits upon a composite surface of the solid tops and the air gaps. This approximation is especially valid since the water droplet size is much bigger than the feature size of nanostructured surface as in the case of our experiments. Therefore, the Cassie and Baxter equation can be applied with two assumptions: first, assuming the shape of nanorods to be a cylinder with pyramidal tips; second, the average contact angle of a flat surface composed of Teflon and Pt portions, where the water completely wets (i.e. no air gaps), is given by

$$\cos \theta_{Y_{Pt-Teflon}} = f_t \cos \theta_t + f_{Pt} \cos \theta_{Pt} \quad (2)$$

where f_t and f_{Pt} are the area fractions of both Teflon and Pt in contact with water and θ_t and θ_{Pt} are the contact angles of flat Teflon and flat Pt surfaces, respectively.

When the water is partially wetting the Pt/Teflon nanorods and there exists air gaps at the bottom between the nanorods, then the Pt/Teflon portion that is in contact with the water will contribute the solid fraction term f_s in equation (1). And, the term θ_Y will be replaced by the final average contact angle of the wetted portion of the Pt/Teflon surface. Therefore, using

equations (1) and (2), the modified Cassie and Baxter equation for our composite nanorods becomes

$$\cos \theta_{CB_{Composite}} = f_{s_{Composite}} \cos \theta_{Y_{Pt-Teflon}} + f_{s_{Composite}} - 1 \quad (3)$$

where $f_{s_{Composite}}$ is the area fraction of solid–liquid (Pt/Teflon portion in contact with water) interfaces. Equation (1) can be used when the water is wetting Teflon only. On the other hand, when the water is wetting both Pt and Teflon, equation (3) can be applied. The fraction of solid–water interface can also be represented in terms of water depth d (figure 5) penetrating into the gaps of nanorods as measured from their tips (e.g. no wetting when water depth is zero and complete wetting when it is equal to the nanorod length):

$$f_s = \frac{2d / \sin \alpha}{[(2d / \sin \alpha) + ((a \tan \alpha - 2d) / \sin \alpha) + b]} \quad (4)$$

$$f_{s_{Composite}} = \{[(2 \times (a/2) \times \tan \alpha) / \sin \alpha] + d - ((a/2) \times \tan \alpha)\} \times \{[(2 \times (a/2) \times \tan \alpha) / \sin \alpha] + d - ((a/2) \times \tan \alpha) + b\}^{-1} \quad (5)$$

$$f_{s_{Composite}} = \{[(2 \times (a/2) \times \tan \alpha) / \sin \alpha] + t\} + [(d - t - ((a/2) \times \tan \alpha))] \times \{[(2 \times (a/2) \times \tan \alpha) / \sin \alpha] + t\} + [(d - t - ((a/2) \times \tan \alpha) + b)]^{-1} \quad (6)$$

where d is the water depth measured from the tip of the nanorods, a is the diameter of the nanorods, b is the gap among the nanorods, t is the Teflon depth measured from the base line of the tip of the nanorods, and α is the tip angle measured from the line parallel to the bottom plane. In our model, the water depth d has been changed in a wide range of values in order to predict the contact angle of the Pt/Teflon composite at different values of d . Hence, different scenarios can be considered. First, Teflon is only at the pyramidal tips of the nanorods and water is partially wetting Teflon only. Therefore, equation (4) can be applied followed by equation (1) to determine the contact angle. In the second case, water is completely wetting Teflon tips and also partially in contact with the Pt base. Hence, after calculating the $f_{s_{Composite}}$ value from equation (5), the contact angle of the Pt/Teflon composite can be calculated using equation (3). Finally, the third scenario assumes that the Teflon, which completely covers the tips of Pt nanorods, partially coats the upper portion of the Pt side walls at the bottom of tips due to the flux angular distribution effect explained above. Similarly, the contact angle in this case can be calculated from equation (3), in which the $f_{s_{Composite}}$ value can be extracted from equation (6).

The tip angle α value of bare Pt nanorods was measured to be about 36° (with respect to the line parallel to the bottom plane) from cross-sectional SEM images. However, one can see that the tip angle of nanorods can be changed due to the presence of Teflon nanopatches which are non-conformally deposited at the tips, especially at longer deposition time. Therefore, we studied the effect of the tip angle on the contact angle of our composite using our modified Cassie–Baxter model. Based on the SEM analysis of our nanorods, we set tip

angle α to 35° , 50° , and 60° , nanorod diameter a to 150 nm, and rod-to-rod gap b to 50 nm in equation (5) and plotted contact angle as a function of water depth d in figure 6(a). In addition, the calculated values of tip height of the nanorods are 56, 63, and 130 nm, corresponding to different tip angles $\alpha = 35^\circ$, 50° , 60° , respectively. It is seen in figure 6(a) that, at a given water depth, the contact angle of Pt/Teflon composite increases as the tip angle of the nanorods increases. In this case, the enhanced contact angle or hydrophobicity is reflected with a decrease in the area fraction of solid–liquid interface for nanorods with sharper tips. In other words, when the water penetration depth is the same, an increase in the tip angle results in an increase in the contact angle. This result is consistent with the Cassie and Baxter theory, which states that for materials with $\theta > 90^\circ$ a decrease in f_s will increase the contact angle. In addition, contact angle values in figure 6(a) are observed to drop rapidly with water depth until the tip height is reached (e.g. $\theta = 134.8^\circ$, 147.4° , and 159.5° at $d = 20$ nm for $\alpha = 35^\circ$, 50° , and 60° , respectively). After that, water starts to form an interface with Pt at the nanorod side walls and contact angle values reduce more slowly with the water depth due to the competition between hydrophilic Pt nanorods and hydrophobic Teflon nanopatches deposited at the tips of Pt nanorods. On top of this, in our modified Cassie–Baxter model, we assumed an average behavior of our nanocomposite depending on the fact that the size of the water droplet is much larger than our composite features. It is important to note that, even in the complete wetting of our composite, where water is in contact with a much larger Pt portion compared to that of Teflon, the contact angle will not be less than 90° , indicating that a small amount of Teflon at the tips of Pt nanorods is able to turn the hydrophilic property of Pt nanorods into a hydrophobic property. According to our experimental contact angle, which is 138° as plotted in figure 6(a), it seems that water is just in contact with Teflon. This can be shown by determining the water depth values for different tip angles corresponding to our experimental contact angle value from figure 6(a), which are as follows: $d = 17$ nm for $\alpha = 35^\circ$, $d = 32$ nm for $\alpha = 50^\circ$, and $d = 48$ nm for $\alpha = 60^\circ$.

In addition to the tip angle, there are also other parameters which may affect the hydrophobic/hydrophilic property of a given surface. For example, let us consider two surfaces having nanorod arrays of the same diameter and tip angle but with different rod-to-rod separation (i.e. different rod-to-rod gap b in figure 5). Let us also assume that both surfaces have the same area fraction of the solid–liquid interface when they are in contact with water. For the nanorods with large spacings, we can still have higher contact angles due to the small f_s , as long as feature spacing is not too large and can support the water droplet surface tension. Hence, in order to better understand the effect of gaps among the nanorods on the contact angle of Pt/Teflon composite, we have changed the value of b in equation (5), which is for the case where Teflon is only at the tips, tip angle is 45° , and nanorod diameter is 150 nm. As expected, figure 6(b) shows that, as the gap among the nanorods increases, the contact angle also increases. This increase in the contact

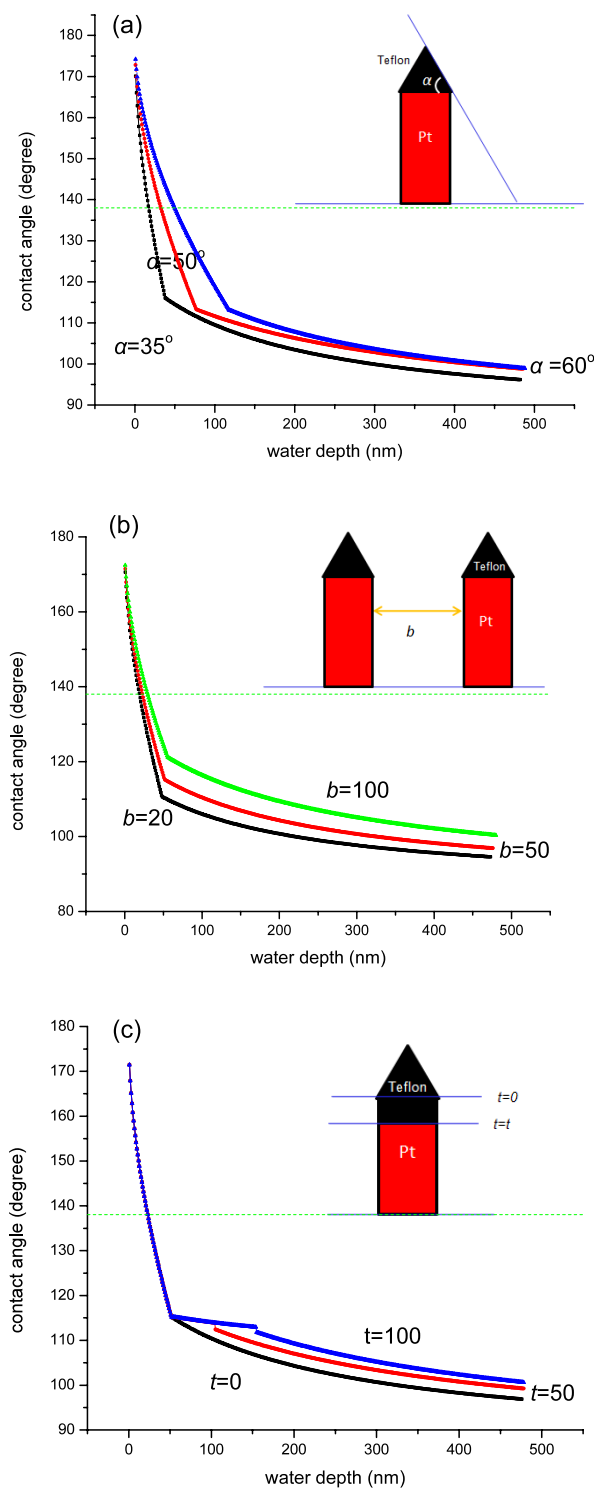


Figure 6. Contact angle values as a function of water penetration depth, as predicted by our wetting model for various values: (a) the tip angle α , (b) nanorod gap b , and (c) the Teflon portion at the Pt nanorod side walls t (apart from the Teflon at the tips).

angle is attributed to the enhanced area fraction of the air beneath the water droplet for nanorods of larger separation as illustrated in figure 6(b). Similar to the tip angle, the effect of gaps among the nanorods has a positive influence on the contact angle and it is consistent with the Cassie and Baxter theory, which states that increasing the area fraction

of the trapped air beneath the water droplet (reducing f_s) results in an increase in the contact angle. Furthermore, our results for the effect of the gaps among the nanorods are further supported by a recent study in which the thermodynamics and kinetics of the transition from the Cassie–Baxter to the Wenzel state has been investigated [25]. In this work, a critical condition for the transition was developed, based on the substrate pattern and intrinsic wetting properties of the substrate material, as follows:

$$b_c = \frac{2h}{\cos \theta + 1} - 2h \quad (7)$$

where b_c is the critical gap size and h is the thickness of the micro/nanostructure surfaces. According to equation (7), if $b_c < b$, no transition is observed. For our case, when $\theta = 138^\circ$, $h = 500$ nm, the calculated critical gap size from equation (7) is about 2894 nm, which is much higher than the spacings (10–100 nm) among our nanocomposite. Hence, in our case, no transition will occur below the critical gap size, which is about 2894 nm. In a similar fashion to the tip angle, our experimental contact angle pointed out in figure 6(b) implies that water is partially wetting Teflon only.

In our experiments, since there is a possibility that an unknown amount of Teflon might have been deposited at the side walls of Pt nanorods due to the angular distribution in the sputter flux, we also studied the effect of the Teflon side wall coating portion (t in figure 5) on the contact angle of the Pt/Teflon nanocomposite. For this we changed the parameter t in equation (6) for nanorods with tip angle $\alpha = 45^\circ$, nanorod diameter $a = 150$ nm, nanorod gap $b = 50$ nm, and plotted predicted contact angle values in figure 6(c). The result in figure 6(c) shows that as the Teflon side wall portion increases the contact angle increase for a given water depth. This is due to the fact that water is in now contact with more Teflon for large value of t compared to the case where Teflon just coated the tips of Pt nanorods. It is important to note that the original Cassie and Baxter model is applied to a single-material solid surface. However, in our case we have Pt/Teflon composite and we considered the average contact angle based on their relative portions that are in contact with water after a surface flattening approximation (figure 5). According to equation (2), the average contact angle of a flat surface composed of Teflon and Pt portions should increase when the Teflon to Pt ratio is increased. As a result, the enhanced average contact angle of a flat surface is expected to lead to an increase in the contact angle of a rough composite material where the water wets partially, according to equation (3). As presented above, our experimental contact angle of the Pt/Teflon composite is about 138° for nanorod coated with GLAD-Teflon. Therefore, according to the result of our model plotted in figure 6, it is predicted that the solid–liquid interface is expected to be mainly at Teflon tips when the composite nanorods are in contact with water.

3.4. Surface energy measurements

Finally, the surface energy calculation on sample 3 (see table 1) was performed using the two-liquid method. In this method

the contact angle of the Teflon, Pt nanorods, and composite was measured using one polar (water) and one non-polar (methylene iodide) liquid. Once the average angles for the sample were determined they were put through a simultaneous equation to determine the surface energy of the sample. The equation used for this is

$$(1 + \cos \theta)\gamma = 2(\gamma^d \gamma_s^d)^{1/2} + 2(\gamma^p \gamma_s^p)^{1/2}. \quad (8)$$

In this equation, the values are as follows: θ is the average angle for the liquid; γ is the surface tension of the liquid, which consists of two parts, γ^d and γ^p , which are the dispersive and polar components respectively of the surface tension of the liquid. The values of γ_s^d and γ_s^p are the dispersive and polar components of the surface energy values of the surface being analyzed. By putting the surface tension values of a polar solution (water) and a non-polar solution (methylene iodide) in this equation, it is possible to solve for the surface energy of the samples. The calculated surface energies were 12.6, 53.35, and 9.25 mN m⁻¹ for bare Teflon film, platinum nanorods, and Pt/Teflon composite, respectively. These values show that the surface energy of the Pt nanorods significantly decreases with addition of Teflon patches on their nanotips; i.e., the higher the contact angle, the lower the surface energy. This result is compatible with the contact angle measurements.

4. Conclusion

We have presented an experimental and theoretical investigation on the wetting of water on a composite nanostructured surface formed by arrays of Pt with Teflon nanopatches. Our Pt/Teflon nanocomposite was fabricated utilizing a sputter glancing angle deposition (GLAD) technique. We have demonstrated that the hydrophilic property of Pt nanostructured surfaces can be turned into highly hydrophobic by adding a small amount of Teflon at the tips of Pt nanorods. The contact angle measurements on this composite have shown contact angle values as high as 138° , indicating a significant increase in the hydrophobicity of originally hydrophilic Pt nanostructures with contact angle value about 52° . We also observed that the GLAD technique is capable of depositing Teflon on selective regions of Pt nanorods, which results in isolated nanostructures. Furthermore, surface energy measurements showed a reduction in the surface energies for our composite Pt/Teflon nanorod arrays. According to our simplified 2D contact angle model, two important findings have been reported: first, it seems that water is more likely to be in contact with Teflon only. Second, even in the case where we have complete wetting (i.e. the water depth is equal to the nanorod length) of our Pt/Teflon nanocomposite, the composite contact angle will not be less than 90° , which indicates the strong hydrophobic effect of Teflon nanopatches on originally hydrophilic Pt nanorods. More detailed modeling studies for describing the hydrophilic/hydrophobic behavior of composite nanostructures are currently under investigation.

Acknowledgment

The authors would like to thank Dr Fumiya Watanabe of the UALR Nanotechnology Center for his valuable support and discussions during SEM measurements.

References

- [1] Choukourov A *et al* 2002 *Surf. Coat. Technol.* **151/152** 214–7
- [2] Bodas D and Gangal A 2005 *J. Micromech. Microeng.* **15** 802–6
- [3] Li L and Zi F 2007 *Mater. Sci. Forum* **561–565** 1229–32
- [4] Harrop R and Harrop P J 1969 *Thin Solid Films* **3** 109
- [5] Morrison D T and Robertson T 1973 *Thin Solid Films* **15** 87–101
- [6] Tibbitt J M, Sten M and Bell T 1975 *Thin Solid Films* **39** L43
- [7] Holland L, Biederman H and Ojha S M 1976 *Thin Solid Films* **35** L19–21
- [8] Biederman H 1981 *Vacuum* **31** 285
- [9] Biederman H 2000 *Vacuum* **59** 594–9
- [10] Biederman H *et al* 2001 *Thin Solid Films* **392** 208–13
- [11] Biederman H *et al* 2003 *Surf. Coat. Technol.* **174/175** 27–32
- [12] Pursel S 2004 *NNIN REU Research Accomplishments* pp 104–5
- [13] Bodas D S, Mandale A B and Gangal S A 2005 *Appl. Surf. Sci.* **245** 202–7
- [14] Satyaprasad A, Jain V and Nema S K 2007 *Appl. Surf. Sci.* **253** 5462–6
- [15] Sakar D K, Farzaneh M and Paynter R W 2008 *Mater. Lett.* **62** 1226–9
- [16] Tadanaga K, Morinaga J and Minami T J 2000 *J. Sol–Gel Sci. Technol.* **19** 211
- [17] Shibuichi S, Yamamoto T, Onda T and Tsujii K 1996 *J. Phys. Chem.* **100** 19512
- [18] Gu C and Zhang T Y 2008 *Langmuir* **24** 12010–6
- [19] Robbie K, Beydaghyan G, Brown T, Dean C, Adams J and Buzea C 2004 *Rev. Sci. Instrum.* **75** 1089
- [20] Karabacak T and Lu T M 2005 *Handbook of Theoretical and Computational Nanotechnology* ed M Rieth and W Schommers (Stevenson Ranch, CA: American Scientific Publishers) chapter 69 p 729
- [21] Karabacak T, Wang G C and Lu T M 2004 *J. Vac. Sci. Technol. A* **22** 1778
- [22] Ye D X, Karabacak T, Wang G C and Lu T M 2005 *Nanotechnology* **16** 1717
- [23] Ye D X, Lu T M and Karabacak T 2008 *Phys. Rev. Lett.* **100** 256102
- [24] Spori D M *et al* 2008 *Langmuir* **24** 5411–7
- [25] Lammertink R, Peters A, Tsai P, Lohse D and Wessling M 2009 *Material Science Research Conf. (San Francisco, April)* Q7, 1